Solvation of HF by Molecular Hydrogen: Helium Nanodroplet Vibrational Spectroscopy†

D. T. Moore and R. E. Miller*

Department of Chemistry, University of North Carolina, Chapel Hill, North Carolina 27599

Received: May 19, 2003; In Final Form: September 2, 2003

The low temperatures and high resolution associated with helium droplet spectroscopy are used to obtain vibrational spectra for clusters containing a single HF molecule, surrounded by multiple H_2, D_2, and HD molecules. For clusters with fewer than nine HD molecules, the asymmetric solvent environment experienced by the HF prevents it from internally rotating. The results suggest that, for $n = 9$ and larger, the solvent cage becomes highly isotropic, allowing the HF molecule to undergo nearly free rotation. For H_2 and D_2 the mixture of ortho and para species in the clusters makes the solvent cage anisotropic even when the first solvent shell is complete and free rotation of the HF molecule is not observed.

Introduction

In recent years there has been growing interest in molecules solvated by molecular hydrogen. For example, a number of techniques have been developed for trapping molecules in solid hydrogen matrixes and recording the associated rovibrational spectra.[1−6] Analyses of the perturbations to the spectrum based on comparison with gas-phase data then provide information about the nature of the solid parahydrogen environment around the dopant. Other groups have generated large clusters (10^3−10^5) of molecular hydrogen in supersonic beams and doped them with atomic[7] and molecular[8] species via a pickup procedure.[9] The doped clusters were then investigated using VUV[7] or infrared[8] spectroscopy, revealing that the dopant species were in a solvated environment. This is in contrast to similar experiments using rare gas clusters, where the dopant molecules adhered to the cluster surfaces.[10] The interpretation was that the hydrogen clusters retain a very high degree of mobility,[7,8] even though the estimated internal temperatures of the clusters (5−9 K) were well below the triple point of molecular hydrogen (13.6 K). A similar experiment on the electronic spectroscopy of alkali metal atoms bound to large hydrogen clusters showed that (as with helium droplets[11]) they are bound to the surface of the clusters, due to their weak interactions with the hydrogen.[12]

More recent infrared spectroscopic studies on even smaller H_2 clusters (<20 molecules) in liquid helium nanodroplets have revealed some fascinating quantum mechanical phenomena.[13−16] In a systematic investigation of size- and isotope- dependent effects on the infrared spectra of OCS−$(H_2/D_2)_n$ ($n = 1$−16) clusters, Toennies and co-workers observed a reduction in the Q-branch intensities for the larger parahydrogen (pH_2) clusters when the temperature was reduced from ∼0.4 K (pure ^{4}He droplets) to ∼0.2 K (mixed ^{3}He/^{4}He droplets). Their interpretation was that this qualitative change heralded the onset of long-range quantum mechanical exchange of parahydrogen molecules, indicating that the solvent shell around the OCS had become superfluid.[17] An earlier path integral Monte Carlo (PIMC) study had predicted significant superfluid character for pure para-H_2 clusters in this size range,[18] and a more recent PIMC study by Kwon and Whaley on $(pH_2)_{17}$–OCS supports the experimental findings of the Toennies group.[19] Whether or not these results conclusively demonstrate superfluidity in a finite parahydrogen cluster remains somewhat controversial. Another experimental study by Moore and Miller using $(HD)_n$−HCN ($n = 1$−14) clusters demonstrated dramatic size-dependent solvation effects on the rotational dynamics of the HCN molecule.[15] Specifically, for clusters with $n < 12$ and $n > 13$, "normal" rovibrational spectra showing P, Q, and R branches were observed. For the $n = 12$ cluster, however, the spectrum consisted only of a single R(0) line ∼3 cm^{-1} to the blue of the vibrational origin, indicating that the HCN was undergoing essentially free rotation inside the isotropic environment of the HD cluster.[15]

A common aspect of the helium droplet experiments reviewed above is that only one structural isomer was observed for a given cluster size in each case.[13,15] This is in contrast to the Ar_n−HF system, where multiple structural isomers were found for cluster sizes greater than $n = 3$.[20] It was further demonstrated that the cluster growth could be controlled by changing the order that the Ar and HF were added to the helium droplets.[20] It is again clear that a large amount of dynamic motion is occurring in the hydrogen clusters, even at the low temperature of the helium droplets (0.37 K [21,22]), allowing them to rearrange into some optimal geometry.

The present study continues this line of research with an investigation of size-dependent trends in the spectroscopy of $(H_2/HD/D_2)_n$−HF clusters in liquid helium nanodroplets. In this work we focus on the vibrational shift of the HF stretching mode in the clusters, using the technique of pendular spectroscopy to simplify the spectra. The rotationally resolved spectra of the clusters will be presented in a future publication.

Experimental Section

The apparatus used in the present study has been discussed in detail previously.[23] The helium droplets are formed by expansion of ultrahigh purity helium through a 5 μm diameter electron microscope pinhole, sealed to the end of a copper tube. This nozzle is cooled to approximately 20 K by a closed cycle helium refrigerator. A silicon diode is used to monitor the nozzle temperature, which is controlled by a feedback system to a heater. The helium gas is precooled in a liquid nitrogen bath and then filtered to prevent blockages of the nozzle by

† Part of the special issue "Charles S. Parmenter Festschrift".

10.1021/jp0306343 CCC: $25.00
Published on Web 10/24/2003

condensable impurities. The source is typically operated at a stagnation pressure of 50 atm, resulting in the formation of helium droplets with an average size of 3700 atoms[24] and a radius of 3.5 nm.[25] The droplets pass through a 10 cm long pickup cell, into which we meter various amounts of HF and H_2 (99.98%), D_2 (98% Cambridge Isotope Laboratories), or HD (97.9% Cambridge Isotope Laboratories). Depending upon the corresponding partial pressures, different numbers of molecules of each kind can be doped into the helium droplets. For all of the experiments discussed here, the HF pressure was optimized for the production of clusters containing a single HF molecule.

Once doped with the molecules of interest, the droplets pass into the multipass cell,[23] where an F-center laser is used to vibrationally excite the H−F stretching mode of the resulting hydrogen−HF binary complex. Subsequent vibrational relaxation of the complex results in the evaporation of several hundred helium atoms, based upon the binding energy of a helium atom to the droplet of ~ 5 cm^{-1}.[26] The corresponding loss in droplet beam energy is then detected by a cryogenically cooled bolometer (Infrared Laboratories) operated at ~1.4 K. In the present study the F-center laser was operated with a KCl:Li crystal (crystal no. 2), pumped by approximately 3 W from a krypton ion laser, yielding approximately 10 mW of output power in the region near 3950 cm^{-1}. A detailed discussion of the scanning and calibration of the laser can be found elsewhere.[27] Relative frequencies were determined to within ±0.0001 cm^{-1} using a temperature stabilized 150 MHz confocal etalon, while the absolute calibration was limited to ±0.01 cm^{-1} by the wavemeter used in this study.

Two electrodes were positioned around the laser interaction region so that a large (~60 kV/cm) dc electric field could be applied for pendular spectroscopy. Details concerning the technique of pendular spectroscopy can be found elsewhere.[28−30] Briefly, the application of sufficiently strong dc fields to polar species results in significant orientation of the permanent dipole moment along the electric field direction. For parallel bands, the rotational fine structure then collapses to a single sharp peak near the vibrational origin,[28] which can aid greatly in simplifying congested spectral regions. A further advantage is that the vibrational chromophore of the oriented complexes has a well-defined direction in the lab frame, so that the excitation laser can be polarized accordingly to maximize the relative orientation.

The 3:1 (2:1) nuclear spin statistics of ortho- and para-H_2 (-D_2) are expected to persist even at the low temperatures of the helium droplets, owing to the extremely slow spontaneous interconversion of the nuclear spins. For some of the experiments reported here, it was helpful to have a hydrogen sample that is enriched in the $J = 0$ species. For this purpose, we used an $Fe(OH)_3$ catalyst (IONEX-type OP), placed in the bottom of a 1/2 in. stainless steel tube that was pressurized with ~800 kPa of hydrogen (99.98%). The tube was then inserted into a liquid helium Dewar so it could be cooled to ~15 K (estimated from the hydrogen vapor pressure). At this temperature, the percentage of para-H_2 is in excess of 99% under equilibrium conditions.[31] The tube was kept at this temperature for at least 3 h before introducing the hydrogen gas into the pickup cell. For some of the experiments discussed here, we used a sample that was somewhat less enriched (due to contamination issues in the warm part of the conversion tube), namely with an para:ortho ratio of approximately 3:1, as measured spectroscopically from the relative intensities of the pendular peaks for the binary complexes of HF with ortho- and para-H_2.

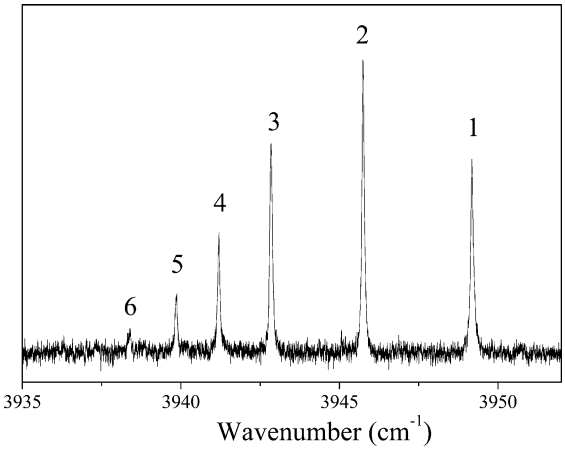

Figure 1. Pendular spectrum of $(HD)_n$−HF clusters. The cluster size n is indicated by the labels over the peaks. The pickup pressures of HF and HD were 1.0×10^{-6} and 2.5×10^{-6} Torr, respectively, and the droplet beam source was set with a helium stagnation pressure of 43 bar and a nozzle temperature of 21.5 K.

TABLE 1: Pendular Peak Positions for $(HD)_n$−HF Clusters (~60 kV/cm Applied Field)[a]

n	1	2	3	4	5	6	7	8
position	49.23	45.75	42.85	41.19	39.86	38.36	37.38	36.30

[a] The values are in cm^{-1} (±0.02 cm^{-1}), and 3900 cm^{-1} has been subtracted from each value for ease of presentation.

Results

$(HD)_n$−HF. We begin by considering $(HD)_n$−HF complexes formed in helium droplets, since this avoids the complexities which arise when multiple nuclear spin species are present. In the case of HD, the nuclear spin symmetry is broken and all of the HD molecules are cooled to $J = 0$. Figure 1 shows a series of pendular peaks obtained with a rather low pressure of HD in the pickup cell and a field strength of 60 kV/cm. As discussed elsewhere,[29] the pendular transitions are used to identify the vibrational origins of the bands. The numbers appearing above each peak in the spectrum refer to the number of HD molecules in the corresponding cluster. The binary complex is easy to assign, since its rotationally resolved, field-free spectrum was measured in a previous study,[32] and the peaks for the larger clusters were assigned based upon the pickup cell pressure dependence of the signals. It is interesting to note that we have obtained very similar data for $(HD)_n$−HCN,[15] which also shows a monotonic increase in the frequency shift with increasing numbers of HD molecules. The observed pendular transition frequencies are summarized in Table 1. In a previous study of the hydrogen−HF binary complexes, we observed that the line width in the HD−HF spectrum was considerably larger than those of the other hydrogen isotopes.[32] We see in Figure 1 that the line widths for all of these complexes are similar, suggesting that the same near resonant vibrational relaxation process proposed for the binary complex (between the HF and HD vibrations) is important in the larger systems as well.[32]

We see that the sequential frequency shifts are all of comparable magnitude, indicating that all of the HD molecules are in the first solvent shell. From previous work on the HF monomer in helium droplets, we know that free HF is only weakly oriented at the field strengths used here, due to its large rotational constant of ~20 cm^{-1}.[33] Therefore, the existence of strong pendular transitions for these $(HD)_n$−HF complexes implies that the HF molecular rotation is "locked" to the end-over-end rotation of the clusters as a whole. As with the earlier

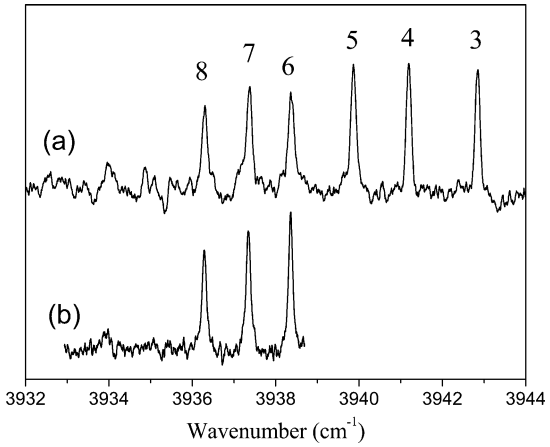

Figure 2. (a) Pendular spectra of larger $(HD)_n-HF$ complexes (HD $= 5.0 \times 10^{-6}$ Torr) in large helium droplets (50 bar and 20 K). The cluster size n is indicated by the labels over the peaks. (b) Same spectrum scanned with a longer time constant to emphasize the weak feature near 3934 cm^{-1} and the sudden cutoff of the spectrum after $n = 8$.

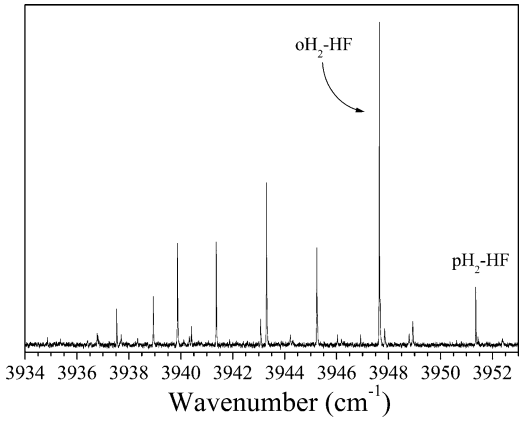

Figure 3. Pendular spectrum of HF (1.2×10^{-6} Torr) with normal H_2 (2.4×10^{-6} Torr), He stagnation pressure of 40 bar, and nozzle temperature of 21 K. Peaks due to the binary clusters are labeled; all other peaks arise from larger clusters.

studies mentioned in the Introduction,[13,15] the observation of only a single band for each cluster size indicates that only one structural isomer is formed in each case, in contrast to observations for heavier systems (Ar_n-HF[20]), where multiple isomers are formed for larger clusters. Apparently the low mass of the HD provides the clusters with sufficient zero-point energy that they are fairly insensitive to local structure in the potential energy surface, indicating that the weak corrugations on the potential energy surface are insufficient to trap the molecules in the corresponding local minima. The picture that emerges for these systems is that the HF is in an anisotropic environment created by the partially filled first solvent shell of HD molecules, but that the anisotropy within the angular range subtended by the solvent molecules is very weak.

As mentioned in the Introduction, the $(HD)_n-HCN$ clusters investigated previously showed similar behavior up to a critical size ($n = 12$), where the solvent cage becomes sufficiently isotropic to allow the HCN molecule to rotate freely.[15] A similar effect is certainly expected for the HF molecule, which has a ~15 times larger rotational constant. To verify this, we carried out experiments at higher HD pressures, as shown by the spectra in Figure 2. Although the pickup pressures used to obtain the spectra were optimized for formation of clusters with more than 10 HD molecules, it is apparent that the progression of peaks in this spectrum suddenly stops at $n = 8$. The implication is that, in analogous fashion to the $n = 12$ case for HCN, the solvent cage in the $n = 9$ complex is sufficiently isotropic that the HF molecule rotates essentially freely within this cage, making the pendular effect much weaker. In contrast with the $(HD)_n-HCN$ system, however, where the addition of further HD molecules produced sufficient anisotropy to once again "lock" the rotation of the HCN to the overall cluster,[15] we see no evidence here for the reappearance of the pendular peaks for larger clusters. There does appear to be a feature near 3934 cm^{-1}, but it is certainly too weak to represent a pendular transition of a cluster with a "locked" HF. This difference from the HCN case can be rationalized to some extent, given that the HF requires a relatively larger anisotropy to prevent its rotation, once again due to the large difference in the rotational constants. Ab initio calculations carried out in our laboratory indicate that the anisotropy of the H_2–HF potential is somewhat greater than for H_2–HCN, confirming that the difference between these two systems is related to the relative sizes of the rotational constants for HF and HCN.

In the $(HD)_n-HCN$ work, the onset of free rotation was characterized by the appearance of a broad R(0) line located 2B (~3 cm^{-1}) to the blue of the vibrational origin.[15] We searched the spectral region from 4010 to 3960 cm^{-1} for evidence of such a feature for the HF complexes, but without success. This is perhaps not too surprising since the $J = 1$ state of HF is known to undergo fast rotational relaxation in helium droplets, which makes the corresponding R(0) transition quite broad and weak.[33] We conclude this section on the HD complexes by noting that one would normally be cautious about overinterpreting a negative result of this type, namely that peaks are missing from the spectrum. However, it will become obvious from the following results for the other isotopes of hydrogen that the HD spectra shown in Figure 2 are indeed anomalous and strongly suggestive of the type of dynamics discussed above.

$(H_2)_n-HF$. Figure 3 shows a pendular spectrum obtained using a moderate pressure of H_2 in the pickup cell and an applied electric field of 60 kV/cm. The peaks near 3951.4 and 3947.6 cm^{-1} are easy to assign, coming very near the vibrational origins of the pH_2–HF and oH_2–HF binary complexes in helium, respectively, as discussed in detail elsewhere.[32] Note also that the intensity ratio is ~3:1, as expected from the relative abundances of ortho- and para-H_2 in normal hydrogen. The peaks to the red of the binary complexes are then assigned to clusters containing more than one hydrogen molecule; however, the pattern of frequency shifts is clearly more complex than for the $(HD)_n-HF$ clusters discussed above. Since oH_2 and pH_2 give rise to significantly different vibrational frequency shifts in the binary complexes, it is reasonable to expect that the frequency shifts for the higher order complexes will depend upon the specific number of ortho- and para-hydrogens in the complex. For example, in the simplest case of $(H_2)_2$–HF there are three possibilities, namely oo, op, and pp, assuming only a single isomer exists for each cluster composition. The number of species then clearly increases with cluster size, accounting for the complexity of the spectrum.

The first step in the assignment of the peaks in the spectrum involves the determination of the cluster sizes (total number of hydrogen molecules in the clusters). Once again, this was done by varying the hydrogen pressure in the pickup cell and recording the resulting variation in the pendular transition intensities. Spectra recorded at three different hydrogen pickup cell pressures are shown in Figure 4. The relative pressure dependences for groups of pendular peaks were then used to

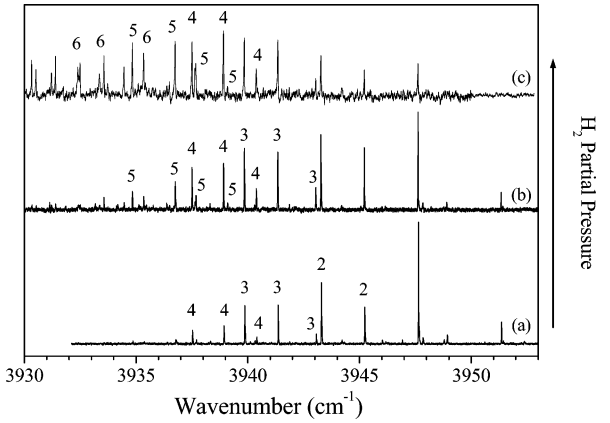

Figure 4. Pendular spectra of $(H_2)_n$−HF clusters at three different pickup pressures of H_2 : (a) 2.4×10^{-6}, (b) 3.3×10^{-6}, and (c) 4.0×10^{-6} Torr. The droplet source conditions (stagnation pressure and nozzle temperature) were 43 bar and 21 K for (a) and (b), and 50 bar and 20 K for (c). The peak labels indicate the number of hydrogen molecules in the cluster responsible for each peak.

determine the total number of hydrogen molecules in the corresponding clusters, as indicated in the figure. The next step was to determine the ortho/para composition for each cluster. Based upon the relative red shifts for the binary complexes, it is expected that clusters containing higher fractions of oH_2 will show larger red shifts. Thus we can tentatively assign the peak furthest to the red in each cluster size manifold to the pure ortho-H_2 cluster. The next most red-shifted peak is then assumed to be due to the cluster with a single para-H_2, and so on.

The relative intensities of the various peaks in these spectra can also be used in the assignment process. As noted above, the experimental intensity ratio for the ortho and para binary complexes is approximately 3:1, consistent with the nuclear spin statistics. This suggests that the transition moment of the HF is not appreciably changed by the hydrogen (or at least the change is approximately the same for ortho- and para-hydrogen). This is certainly consistent with the weakness of the interactions in these systems.[34] These statistics are easily extended to larger clusters to obtain an estimate of the expected relative intensities in the pendular spectrum. For example, the expected intensity pattern for the $n = 2$ clusters is 9:6:1 for the oo:op:pp clusters, respectively, where we assume that there is only one isomer for each cluster composition (i.e., op = po). These intensity ratios are in excellent agreement with the experimental pendular peak intensities seen in Figure 4. For the $n = 3$ clusters, the observed intensities again fit the ooo:oop:opp:ppp ratios of 27:27:9:1 that are expected in the absence of structural isomers. Maintaining the assumption that only a single peak exists per ortho/para composition, we can derive the following general expression for the relative abundances of clusters with a given size n, as a function of the number of ortho molecules, k:

$$a_n(k) = \frac{d^k}{M^n} \frac{n!}{k!(n-k)!} \qquad (1)$$

where d is the relative abundance of the ortho species (3 for H_2 and 2 for D_2), relative to the total abundance M (4 for H_2 and 3 for D_2).

Since para-H_2 is in low natural abundance, clusters with large numbers of parahydrogen are not observed in the pendular spectra. This problem was overcome by using para-enriched hydrogen, as shown in Figure 5, where the spectra obtained with normal H_2 and para-enriched H_2 (75% para abundance) are compared. Clusters containing large numbers of para-H_2 are

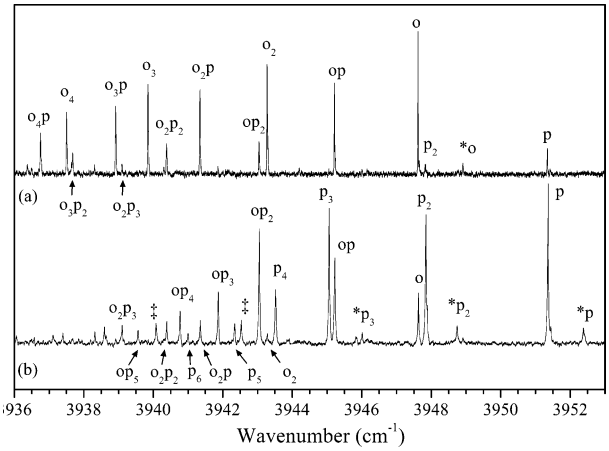

Figure 5. Pendular spectra of $(H_2)_n$−HF clusters recorded using (a) normal H_2 (3:1 ortho:para abundance) and (b) para-enriched H_2 (1:3 ortho:para abundance). The droplet source conditions (45 bar and 22.5 K) and pickup pressures (HF = 1.2×10^{-6} Torr, $H_2 = 2.3 \times 10^{-6}$ Torr) used to record the spectra were the same. Peaks are labeled by composition using the notation o_jp_k. The peaks labeled with an asterisk (*) have the same pressure dependence as the main peak and are tentatively assigned as "pendular satellites" (see text).. Peaks labeled with a double dagger (‡) were not reproducible from day to day and are therefore due to an unknown impurity.

TABLE 2: Peak Positions for Pendular Transitions (∼60 kV/cm Applied Field) of $(H_2)_n$−HF Clusters with n Total Hydrogens and k Ortho H_2's[a]

	n						
k	1	2	3	4	5	6	7
0	51.37	47.85	45.05	43.52	42.33	40.99	40.11
1	47.62	45.21	43.05	41.87	40.77	39.55	38.57
2		43.28	41.34	40.38	39.10	37.84	37.38
3			39.85	38.92	37.68	36.49	35.72
4				37.50	36.75	35.36	34.46
5					34.85	33.59	32.49
6						32.40	31.40
7							30.52

[a] The values are in cm^{-1}(± 0.01 cm^{-1}), and 3900 cm^{-1} has been subtracted from each value for ease of presentation. For example, the position for the cluster with $n = 5$ and three oH_2 molecules is 3937.68 cm^{-1}.

now clearly visible in the spectrum. The analysis of the intensity patterns for both sets of data provides us with firm assignments of all the possible combinations for clusters with $n \leq 7$, some of which are indicated in Figure 5 using the notation o_jp_k, to denote a cluster with j ortho- and k para-H_2 molecules. A complete list of the transition frequencies, along with their assignments, is given in Table 2. Looking at the collected data, we see that our assumption of one peak per spin composition of the clusters is quite well justified. While this is not particularly remarkable for the $n = 2$ and $n = 3$ clusters, the fact that this behavior persists up to at least $n = 7$ is again an indication that the dynamical motion between the various local minima on the surface occurs faster than the time scale of the present experiment.

An additional point of interest in Figures 4 and 5 is the presence of weak features located ∼1 cm^{-1} to the blue of the main pendular peaks for some of the smaller clusters. There features have the same pickup pressure dependence as the primary pendular peaks. These peaks could be associated with some minor isomer formed in the droplets, although we do not have a firm assignment for them at this time.

Figure 6 shows plots of the frequency shifts (from the vibrational origin of the free HF in ^{4}He droplets, namely

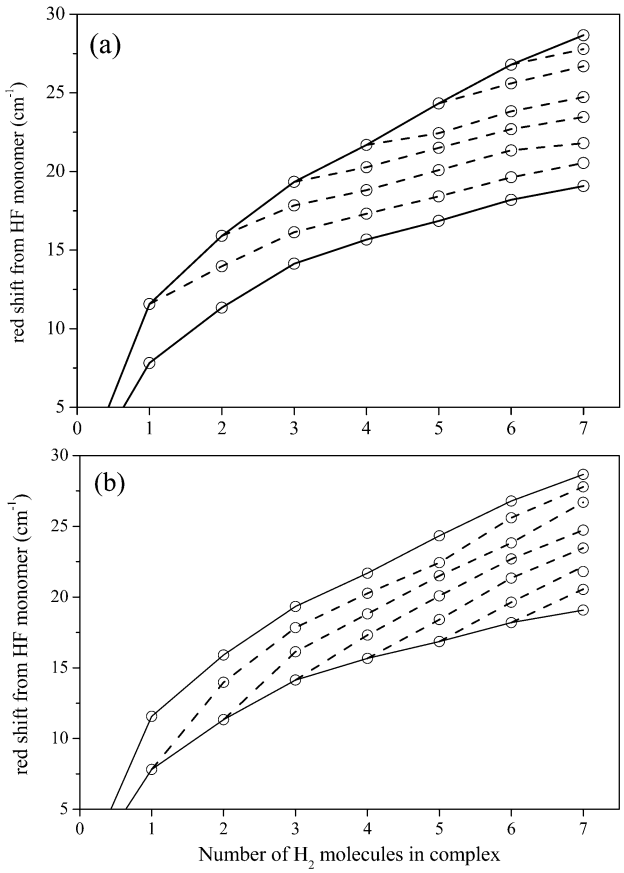

Figure 6. Pendular red shift data for all of the $(H_2)_n$−HF clusters as a function of cluster size and composition. Closed circles denote pure ortho-H_2 clusters, closed squares denote pure para-H_2 clusters, and open triangles denote clusters with a mixed ortho−para composition. The data in the two plots is the same; however, the dashed lines in (a) track the red shifts for clusters with a fixed number of ortho-H_2 molecules, while the dashed lines in (b) track the red shifts for clusters with a fixed number of para-H_2 molecules (see text.)

3959.186 cm^{-1} [33]) as a function of the cluster size (same data in both graphs, only the connecting lines are different). As expected, the clusters consisting of pure orthohydrogen have the largest shifts for a given cluster size, while the pure parahydrogen clusters have the smallest shifts. In both cases the regular trend in the incremental shifts indicates that all of the molecules are accumulating in the first solvent shell, as was observed for HD. Clusters with mixed compositions lie between the curves for the pure ortho and pure para clusters, and while the distribution is fairly even, there are some "irregularities" that give clues about structural trends in the clusters. To emphasize these trends, we have added different sets of dashed lines through the data in Figure 6a and 6b, tracking clusters with fixed numbers of ortho-H_2 and para-H_2 molecules, respectively. In Figure 6a, the spacings between the dashed lines remain fairly constant with increasing cluster size, indicating that the effect of adding, say, four para-H_2 molecules to a pure ortho cluster is independent of the size of the ortho cluster. Furthermore, the shifts associated with adding successive pH_2 molecules for a given ortho cluster are quite similar. This suggests that the oH_2 molecules, which have stronger interactions with the HF,[34,35] find their optimal arrangement, leaving the pH_2 molecules to fit in around them as best they can.

This same trend is also evident in Figure 6b, where the jagged nature of the lines makes it clear that the addition of subsequent ortho-H_2 molecules can have quite different effects on the red

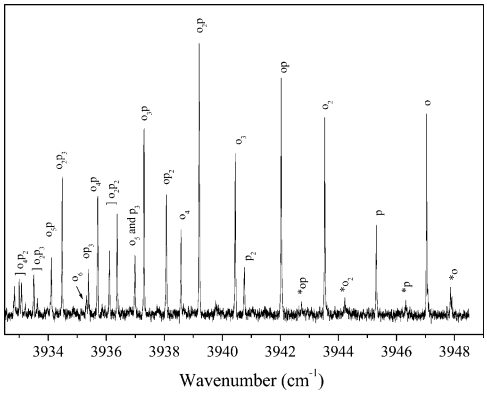

Figure 7. Pendular spectrum of $(D_2)_n$−HF clusters. The peaks are labeled according to their ortho/para composition in analogous fashion to the $(H_2)_n$−HF clusters. The pickup pressures of HF and D_2 were 1.0 × 10^{-6} and 3.5 × 10^{-6} Torr, respectively, and the droplet beam source was set with a helium stagnation pressure of 45 bar and a nozzle temperature of 20.5 K.

TABLE 3: Peak Positions for Pendular Transitions (∼60 kV/cm Applied Field) of $(D_2)_n$−HF Clusters with *n* Total Deuteriums and *k* Para D_2's[a]

	n					
k	1	2	3	4	5	6
0	47.04	43.52	40.43	38.56	36.98	35.33
1	45.30	42.02	39.19	37.29	35.70	34.09
2		40.73	38.06	36.37	34.47	33.09
3			37.00	35.36	33.62	
2 (iso)[b]				36.10		33.00
3 (iso)[b]					33.5	

[a] The values are in cm^{-1} (±0.01 cm^{-1}), and 3900 cm^{-1} has been subtracted from each value for ease of presentation. For example, the position for the cluster with $n = 3$ and one pD_2 molecule is 3939.19 cm^{-1}. [b] Second structural isomer (see text).

shift for the clusters. In particular, it is clear (also from Figure 6a) that the shift associated with the addition of the fifth ortho-H_2 molecule is significantly larger than any of the others. This suggests additional complexity in the forces driving the aggregation process, perhaps reflecting the presence of the extra quadrupole−quadrupole interaction in the oH_2−oH_2 potential. In any case, it is quite clear that the ortho-H_2 molecules play a more dominant role in determining the cluster structures. More precise information about the structures can be obtained from the rotationally resolved spectra, which will be the subject of a future publication.

$(D_2)_n$−HF. Figure 7 shows a pendular spectrum for HF−$(D_2)_n$, recorded with a moderate pickup pressure of D_2. Once again the two peaks at the high-frequency end of the spectrum are known to come from the binary clusters,[32] and the bands further to the red can be assigned using the approach laid out above. In this case the appropriate nuclear spin weights are 2:1 for ortho:para. Since the $J = 0$ species ortho-D_2 is already more abundant under normal conditions, the population enhancement produced by spin conversion does not provide much assistance in the peak assignments. As a result, some of the complexes are not observed for $n > 3$, as is evident in Table 3.

Upon careful examination of these data, we found that the pattern of peaks is even more complex than that for normal hydrogen. For the $n = 3$ complexes we observed the four bands expected in the one-peak-per-composition limit (o_3, o_2p, op_2, and p_3), with relative intensities as predicted by eq 1. However, beyond this point the one-peak-per-composition assumption breaks down—there are simply too many peaks present and the observed intensity ratios do not match the predictions from eq

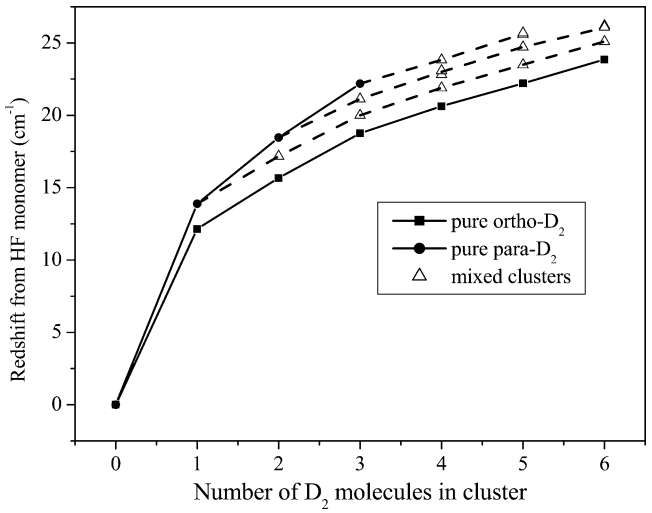

Figure 8. Incremental red shift curves for $(D_2)_n$−HF clusters as a function of cluster size *n*. The dashed curves indicate incremental shifts for clusters with a fixed number of para-D_2 molecules. The doubled symbols (for o_2p_2, o_2p_3, and o_4p_2 clusters) reflect systems with structural isomers (see text).

1. Nevertheless, after careful analysis of the pressure dependence, we determined that, by assigning "doubled" peaks to just three compositions (o_2p_2, o_2p_3, and o_4p_2), all of the observed transitions for clusters up to $n = 6$ could be unambiguously assigned. This assignment is justified based on the fact that the separations between the "doubled" peaks are small, and that the additive intensities of the doublets bring the total intensity distributions for the $n = 4-6$ cluster size manifolds into agreement with eq 1.

The most obvious explanation for these observed peak doublings is that more than one structural isomer exists for these cases. The lower zero-point energy of these D_2 complexes, compared to the lighter isotopes, may make the barriers between the various local minima high enough to prevent rearrangement from one isomer to another. Alternatively, the doubling observed in the spectrum could be due to some form of tunneling dynamics. Unfortunately, the spectra reported here do not provide sufficient information to allow us to differentiate between these two explanations. Pump−probe experiments could be used to help in differentiating between these two possibilities.

Figure 8 shows a plot of the vibrational frequency shifts for the $(D_2)_n$−HF complexes. The dashed lines emphasize the incremental shifts for clusters with fixed numbers of para-D_2 molecules. Comparisons with the analogous results for H_2 reveal another important effect of the difference in the zero-point energies. Although the curves for the two isotopes are quite similar, the differences between the shifts associated with the addition of ortho-D_2 and para-D_2 are much smaller than those for H_2. This can be rationalized by noting that the difference between the binding energies (D_0's) of the ortho and para nuclear spin species to HF is smaller for D_2 than for H_2, due to zero point energy effects.[34] The zero point energy effects on the shifts can be further appreciated from the plot in Figure 9, where only the $J = 0$ isotopic species are shown, namely $(pH_2)_n$−HF, $(HD)_n$−HF, and $(oD_2)_n$−HF. For a given cluster size the red shifts get progressively larger with increasing isotopic mass, as do the incremental shifts between adjacent clusters. This behavior is consistent with the expected trend in the binding energies of the clusters based on elementary zero-point arguments.

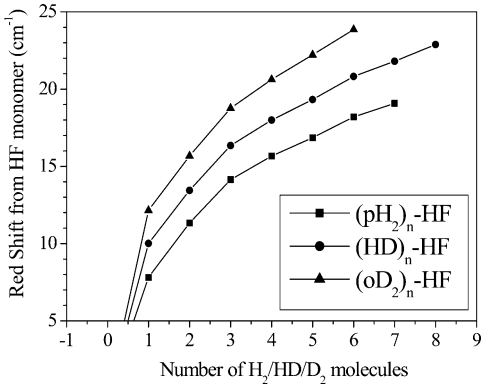

Figure 9. Cluster size dependent red shifts for clusters of $J = 0$ hydrogen molecules with HF.

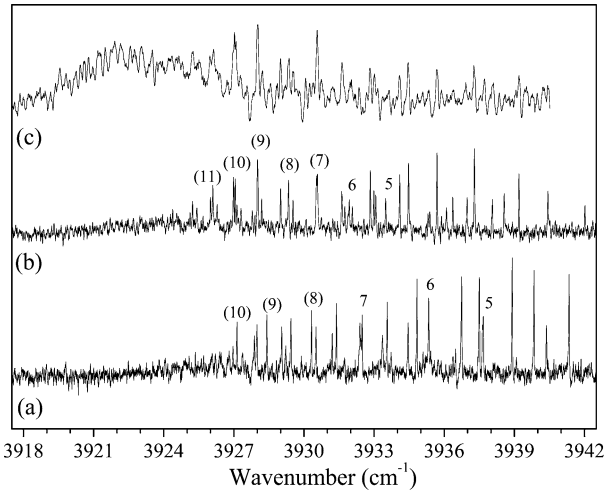

Figure 10. (a) Pendular spectrum of $(H_2)_n$−HF clusters recorded with high pickup pressure of H_2 (5.0×10^{-6} Torr). The labeled peaks are assigned to clusters containing two pH_2 molecules, with extrapolated assignments indicated in parentheses (see text). (b) Pendular spectrum of $(D_2)_n$−HF clusters recorded using similar pickup pressures and droplet beam conditions (50 bar and 20 K). The labeled peaks are assigned to clusters containing three pD_2 molecules, with extrapolated assignments indicated in parentheses (see text). (c) Pendular spectrum of $(D_2)_n$−HF clusters recorded using higher pickup pressure (7.4×10^{-6} Torr) and larger droplets (70 bar and 20 K).

Larger Clusters: Solvation of HF by Hydrogen. In the sections above, we focused on smaller clusters, where the assignments of the size and the composition are secure. Figure 10 shows pendular spectra for $(H_2)_n$−HF and $(D_2)_n$−HF recorded at high pickup cell pressures using large droplets in order to make even larger clusters. Although the assignments become somewhat less clear due to the very large number of cluster compositions that exist for each value of *n*, these clusters are of considerable interest given that they span the size range corresponding to the completion of the first solvent shell. It is important to point out that the conditions used to obtain the spectra in Figure 10 were similar to those used for the $(HD)_n$−HF spectra shown in Figure 2.

To obtain estimates of the largest cluster sizes reflected in these spectra, we used extrapolation based on the red-shift trends shown in Figures 6 and 8, and abundances predicted using eq 1. In the case of H_2 (Figure 10a), the most abundant compositions for $n = 8-11$ are the ones containing only two pH_2 molecules. The labels in Figure 10a thus show the assigned peaks for $n = 5-7$ for clusters with two pH_2's, with the extrapolated assignments for larger clusters (up to $n = 10$) indicated in parentheses. For D_2 (Figure 10b), the most abundant

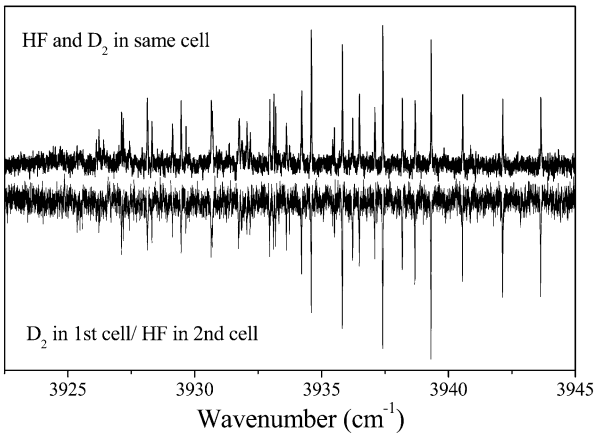

Figure 11. Pickup order dependences of $(D_2)_n-$HF pendular spectra. The inverted spectra were recorded with the D_2 added to the droplet before the HF in a separate pickup cell. The experimental conditions (D_2 pickup pressure, helium stagnation pressure, and nozzle temperature) used for the scan were 4.6×10^{-6} Torr, 50 bar, and 20 K.

compositions predicted for $n = 7-11$ clusters are those containing three pD_2 molecules. Thus the most intense peaks in the spectrum in Figure 10b were extrapolated based on the assignments of the $n = 5-6$ clusters with three pD_2's. From these extrapolations, we see that clusters containing at least 10−11 hydrogen molecules (for both H_2 and D_2) are observed to have strong pendular spectra.

Figure 10c shows a spectrum obtained with even larger droplets and higher D_2 pickup cell pressures. We now observe that the progression of pendular peaks terminates into a broad feature. This is consistent with the formation of clusters with D_2 molecules in the second solvent shell, where the corresponding frequency shifts are much smaller, resulting in strongly overlapping bands that give rise to the broad feature observed here. It is important to note that this broad feature exhibits a strong pendular effect, indicating that the HF molecule is "locked" in the cage of deuterium. This behavior is to be contrasted with the $(HD)_n-$HF system discussed above, where the pendular spectrum suddenly terminated after $n = 8$. The implication is that the solvent environments in the H_2 and D_2 clusters are much more anisotropic than in HD, presumably because of the mixed ortho/para compositions of the former systems.

In closing, we present data on the pickup order dependence of the $(D_2)_n-$HF spectra. In the case of the $(Ar)_n-$HF clusters, when the HF was added to droplets already containing (fully cooled) argon clusters, it bound exclusively to the surfaces of the clusters. In the opposite case, when HF was added to the droplets before argon, the argon atoms solvated the HF molecule.[20] The implication was that the preformed argon clusters were quite rigid, so that even though the structures with a "solvated" HF were lower in energy, the system did not rearrange.[20] Figure 11 compares two pendular spectra of $(D_2)_n-$HF clusters, one resulting from the pickup of D_2 first, and then HF, and the other with the two gases in the same pickup cell. Clearly, the spectra are essentially identical up to the largest cluster sizes, indicating that the same clusters are formed irrespective of the order of pickup. This provides one last point in support of the already well-established conclusion that these hydrogen clusters are quite dynamic, and maintain the ability to efficiently rearrange, even up to quite large ($n \sim 12$) cluster sizes.

Summary

We have presented systematic studies of size-dependent trends in the pendular spectroscopy of HF in clusters composed of isotopomers of molecular hydrogen (H_2, HD, D_2). In the most straightforward situation with the $(HD)_n-$HF clusters, where nuclear spin statistics do not play a role, a sequence of strong pendular peaks with monotonically increasing red shifts was observed. Based on the pickup pressure dependence, the peaks were assigned to clusters with sizes up to $n = 8$, with a single peak observed for each different size. For HF in clusters of H_2 and D_2 the situation is somewhat more complicated due to the existence of distinct ortho and para nuclear spin species for these molecules, which allow the formation of several different compositions for a given size. Nevertheless, using a combination of the pickup pressures and the predicted relative abundances of the different ortho/para compositions, unambiguous assignments were determined for cluster sizes up to $n = 7$ for H_2 and $n = 6$ for D_2. From the trends in the incremental red shifts, it is clear that all of the molecules go in the first solvent shell, and almost without exception, only one pendular peak is observed for each cluster composition. This is an indication of a high degree of mobility within the clusters since the cluster aggregation in the helium droplets is a statistical process. In addition, identical spectra are observed for the $(D_2)_n-$HF clusters when the HF and D_2 are picked up in different cells, providing further support for the picture of a highly dynamic environment within the hydrogen clusters.

Spectra were also obtained for even larger clusters, with an aim toward determining the number of molecules in the first solvent shell. For the H_2 and D_2 clusters, well-resolved spectral features are observed for cluster sizes up to $n \sim 10-11$, at which point they coalesce into a single broad peak. This behavior strongly suggests that the first solvent shell of these clusters contains approximately 10−11 H_2/D_2 molecules. Sharply contrasting behavior is observed for the $(HD)_n-$HF clusters, where no matter how high the HD pickup pressure is increased, no strong pendular features are observed for clusters larger than $n = 8$. By analogy with our previous study on $(HD)_n-$HCN clusters,[15] our conclusion was that for clusters with $n \approx 9$, the solvation environment becomes sufficiently isotropic that the HF molecule can undergo free rotation within the cluster.

Clusters of pure parahydrogen are clearly of considerable interest given the recent evidence of superfluidity in such systems.[13,19] Unfortunately, the conversion apparatus used for the current experiments could not supply para-H_2 with the high purities (>98%) required for such work. Improvements to the apparatus are under way, and spectra of HF in pure parahydrogen clusters will be the subject of a future publication.

Acknowledgment. Support for this research from the National Science Foundation (CHE-99-87740) and the Air Force Office of Scientific Research (AFOSR) is gratefully acknowledged.

References and Notes

(1) Momose, T.; Shida, T. *Bull. Chem. Soc. Jpn.* **1998**, *71*, 1.
(2) Fajardo, M. E.; Tam, S. *J. Chem. Phys.* **1998**, *108*, 4237.
(3) Momose, T.; Katsuki, H.; Hoshina, H.; Sogoshi, N. *J. Chem. Phys.* **1997**, *107*, 7717.
(4) Fajardo, M. E.; Tam, S. *J. Chem. Phys.* **2001**, *115*, 6807.
(5) Anderson, D. T.; Hinde, R. J.; Tam, S.; Fajardo, M. E. *J. Chem. Phys.* **2002**, *116*, 594.
(6) Baiocchi, F. A.; Dixon, T. A.; Klemperer, W. *J. Chem. Phys.* **1982**, *77*, 1632.
(7) von Haeften, K.; Laarmann, T.; Wabnitz, H.; Moller, T. *J. Electron. Spectrosc.* **2000**, *106*, 199.

(8) Goyal, S.; Schutt, D. L.; Scoles, G.; Robinson, G. N. *Chem. Phys. Lett.* **1992**, *196*, 123.
(9) Gough, T. E.; Mengel, M.; Rowntree, P.; Scoles, G. *Proc. SPIE-Int. Soc. Opt. Eng.* **1986**, *669*, 129.
(10) Goyal, S.; Robinson, G. N.; Schutt, D. L.; Scoles, G. *J. Phys. Chem.* **1991**, *95*, 4186.
(11) Stienkemeier, F.; Higgins, J.; Ernst, W. E.; Scoles, G. *Phys. Rev. Lett.* **1995**, *74*, 3592.
(12) Callegari, C.; Higgins, J.; Stienkemeier, F.; Scoles, G. *J. Phys. Chem. A* **1998**, *102*, 95.
(13) Grebenev, S.; Sartakov, B.; Toennies, J. P.; Vilesov, A. F. *Science* **2000**, *280*, 1532.
(14) Grebenev, S.; Lugovoj, E.; Sartakov, B.; Toennies, J. P.; Vilesov, A. F. *Faraday Discuss.* **2001**, 118.
(15) Moore, D. T.; Miller, R. E. *J. Chem. Phys.* **2003**, *119*, 4713.
(16) Grebenev, S.; Sartakov, B.; Toennies, J. P.; Vilesov, A. F. *Phys. Rev. Lett.* **2003**, *89*, 225301-1.
(17) Grebenev, S.; Sartakov, B.; Toennies, J. P.; Vilesov, A. F. *Science* **2000**, *280*, 1532.
(18) Sindzingre, P.; Ceperley, D. M.; Klein, M. L. *Phys. Rev. Lett.* **1991**, *67*, 1871.
(19) Kwon, Y.; Whaley, K. B. *Phys. Rev. Lett.* **2003**, *89*, 273401-1.
(20) Nauta, K.; Miller, R. E. *J. Chem. Phys.* **2001**, *115*, 10138.
(21) Hartmann, M.; Miller, R. E.; Toennies, J. P.; Vilesov, A. F. *Phys. Rev. Lett.* **1995**, *75*, 1566.
(22) Brink, D. M.; Stringari, S. *Z. Phys. D* **1990**, *15*, 257.
(23) Nauta, K.; Miller, R. E. *J. Chem. Phys.* **1999**, *111*, 3426.
(24) Knuth, E. L.; Schilling, B.; Toennies, J. P. *19th International Symposium on Rarefied Gas Dynamics*; 1995; p 270.
(25) Lewerenz, M.; Schilling, B.; Toennies, J. P. *Chem. Phys. Lett.* **1993**, *206*, 381.
(26) Brink, D. M.; Stringari, S. *Z. Phys. D* **1990**, *15*, 257.
(27) Huang, Z. S.; Jucks, K. W.; Miller, R. E. *J. Chem. Phys.* **1986**, *85*, 3338.
(28) Block, P. A.; Bohac, E. J.; Miller, R. E. *Phys. Rev. Lett.* **1992**, *68*, 1303.
(29) Rost, J. M.; Griffin, J. C.; Friedrich, B.; Herschbach, D. R. *Phys. Rev. Lett.* **1992**, *68*, 1299.
(30) Moore, D. T.; Oudejans, L.; Miller, R. E. *J. Chem. Phys.* **1999**, *110*, 197.
(31) Younglove, B. A. *J. Phys. Chem. Ref. Data* **1982**, *11*, 1−97.
(32) Moore, D. T.; Miller, R. E. *J. Chem. Phys.* **2003**, *118*, 9629.
(33) Nauta, K.; Miller, R. E. *J. Chem. Phys.* **2000**, *113*, 9466.
(34) Clary, D. C.; Knowles, P. J. *J. Chem. Phys.* **1990**, *93*, 6334.
(35) Lovejoy, C. M.; Nelson, D. D., Jr.; Nesbitt, D. J. *J. Chem. Phys.* **1987**, *87*, 5621.